JACS
JOURNAL OF THE AMERICAN CHEMICAL SOCIETY

Communication

pubs.acs.org/JACS

Rh-Catalyzed (5+2) Cycloadditions of 3-Acyloxy-1,4-enynes and Alkynes: Computational Study of Mechanism, Reactivity, and Regioselectivity

Xiufang Xu,*[,†,‡] Peng Liu,[‡] Xing-zhong Shu,[§] Weiping Tang,*[,§] and K. N. Houk*[,‡]

[†]Department of Chemistry, Nankai University, Tianjin, 300071, P.R. China

[‡]Department of Chemistry and Biochemistry, University of California, Los Angeles, California 90095-1569, United States

[§]School of Pharmacy and Department of Chemistry, University of Wisconsin, Madison, Wisconsin 53705-2222, United States

Supporting Information

ABSTRACT: The mechanism of Rh-catalyzed (5+2) cycloadditions of 3-acyloxy-1,4-enyne (ACE) and alkynes is investigated using density functional theory calculations. The catalytic cycle involves 1,2-acyloxy migration, alkyne insertion, and reductive elimination to form the cycloheptatriene product. In contrast to the (5+2) cycloadditions with vinylcyclopropanes (VCPs), in which alkyne inserts into a rhodium−allyl bond, alkyne insertion into a Rh−C(sp^2) bond is preferred. The 1,2-acyloxy migration is found to be the rate-determining step of the catalytic cycle. The electron-rich *p*-dimethylaminobenzoate substrate promotes 1,2-acyloxy migration and significantly increases the reactivity. In the regioselectivity-determining alkyne insertion step, the alkyne substituent prefers to be distal to the forming C−C bond and thus distal to the OAc group in the product.

Seven-membered carbocycles have attracted increasing interest in natural product synthesis and pharmaceutical chemistry.[1] In contrast to the facile synthetic routes to 5- and 6-membered rings, efficient cycloaddition strategies to form 7-membered rings, such as (5+2) and (4+3) reactions, are limited.[2] In 1995, the Wender group reported the first transition metal (TM)-catalyzed (5+2) cycloadditions employing vinylcyclopropanes (VCPs) as the 5-carbon synthon. This methodology has evolved to a general and effective route to 7-membered rings.[3] A variety of (5+2) cycloadditions of VCPs and 2π systems with different TM catalysts were developed by Wender,[4] Trost,[5] Louie,[6] Fürstner,[7] Yu,[8] Mukai,[9] and others.[10] Stryker[11] and Tanino[12] also reported different types of (5+2) cycloadditions using stoichiometric amounts of metals. The Houk group, along with Wender and Yu, explored the detailed mechanism of the VCP cycloadditions with Rh catalysts using computations.[13] Recently, the Tang group reported a new class of (5+2) cycloadditions using 3-acyloxy-1,4-enyne (ACE) in place of VCP as 5-C synthon.[14] This methodology provides a direct route to 7-membered rings with three C=C double bonds that could be selectively functionalized (Scheme 1). Both intra- and intermolecular cycloadditions have been achieved to produce various substituted cyclic compounds from ACEs and readily available terminal or internal alkynes.

Scheme 1. Rh-Catalyzed (5+2) Cycloadditions of 3-Acyloxy-1,4-enyne and Alkynes

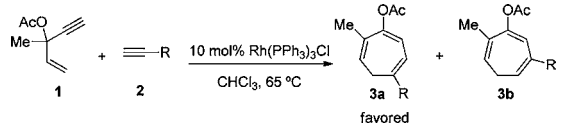

Scheme 2. Proposed Mechanisms of Rh-Catalyzed (5+2) Cycloadditions of (a) ACE amd (b) VCP and Alkynes

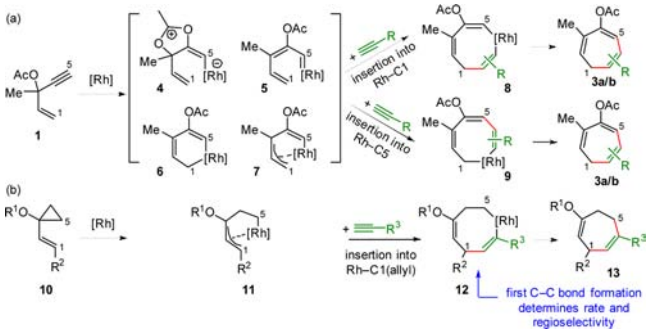

In contrast to the detailed computational and mechanistic studies on the (5+2) cycloadditions with VCPs,[13] the mechanism of the reaction with ACE remains unclear. In previous experimental studies, we proposed a mechanism involving 1,2-acyloxy migration of ACE via possible intermediates **4**−**7** (Scheme 2a).[15] Subsequent alkyne insertion into the Rh−C bond and reductive elimination afford the cycloadduct. The (5+2) cycloadditions with VCPs involve the formation of rhodium-allyl complex **11**, in close analogy to one of the possible intermediates (**7**) in the reaction with ACE, alkynes insertion, and reductive elimination (Scheme 2b). Although the formation of the intermediate **7** is much more complicated than that of Rh-allyl complex **11**, the latter half of the proposed mechanism in Scheme 2a appears to be similar to the (5+2) cycloaddition with VCP in Scheme 2b. The alkyne insertion into complex **11** takes place at the Rh−allyl bond (C1) and forms the first C−C bond with the terminal alkenyl C of VCP. The Xu, Houk, and Tang groups have now worked together to explore the mechanisms of

Received: April 12, 2013
Published: May 31, 2013

dx.doi.org/10.1021/ja4036785 | *J. Am. Chem. Soc.* 2013, 135, 9271−9274

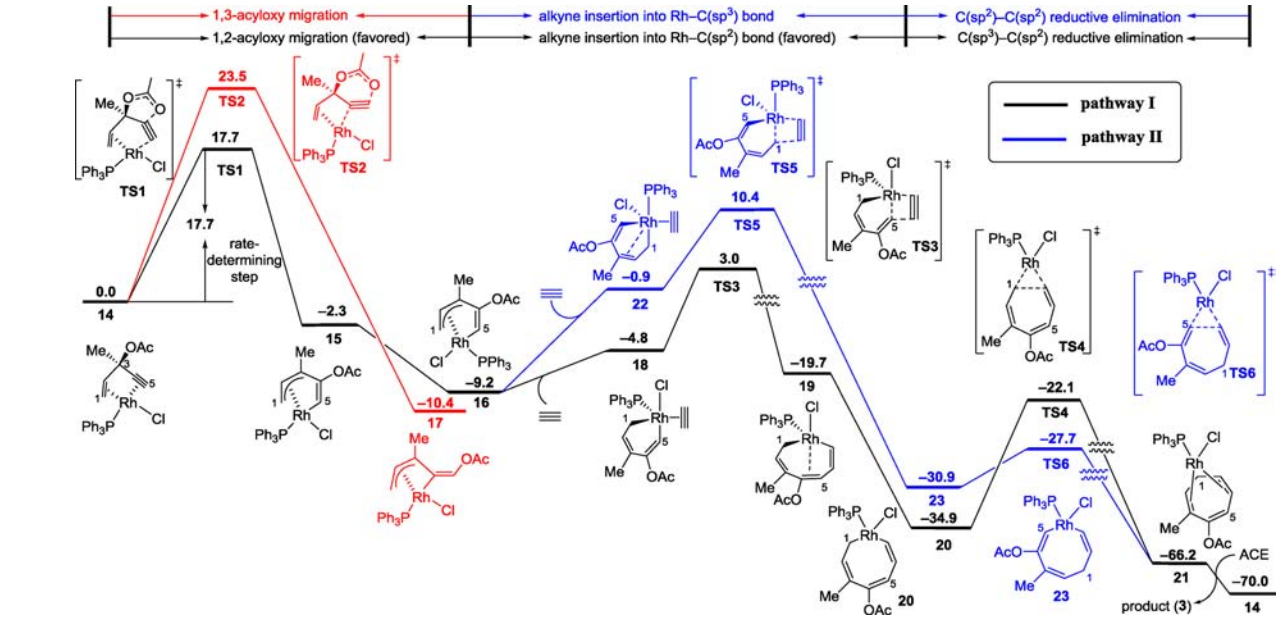

Figure 1. Gibbs free energy profile of the $Rh(PPh_3)_3Cl$-catalyzed (5+2) cycloaddition of ACE and acetylene. Energies are in kcal/mol and calculated using M06/SDD-6-311+G(d,p)/SMD($CHCl_3$)//B3LYP/SDD-6-31G(d)/SMD($CHCl_3$).

the (5+2) cycloadditions involving the new 5-C building block—ACE. The DFT investigations described here reveal several fundamental differences in the nature of rate- and regioselectivity-determining steps, and the order of formation of the two new C−C bonds, when employing ACE in place of VCP as the 5-C synthon. The change of mechanism results in different regiochemical control as well as unique substituent effects on reactivity.

The computed Gibbs free energy profiles of several possible reaction pathways of $Rh(PPh_3)_3Cl$-catalyzed reaction of ACE and acetylene are shown in Figure 1. Geometry optimization and frequency analysis were performed in $CHCl_3$ solvent with the SMD solvation model using B3LYP and a mixed basis set of SDD for Rh and 6-31G(d) for other atoms. Single-point energies were calculated at the M06/6-311+G(d,p) level (SDD for Rh) with the SMD solvation model ($CHCl_3$ solvent) on B3LYP-optimized geometries. All calculations were carried out with Gaussian 09.[16] Entropic contributions to the reported free energies were calculated from partition functions evaluated using Truhlar's quasiharmonic approximation.[17]

In the presence of π-acidic TM catalysts, terminal propargylic esters undergo 1,2-acyloxy migration, while internal propargylic esters undergo 1,3-migration.[18] Previous computational studies indicated Au and Pt catalysts promote the 1,2-acyloxy migration of ACE via a stepwise mechanism involving intermediates similar to **4**.[19] We investigated the 1,2- and 1,3-acyloxy migration pathways with ACE. The reaction initiates from the ACE-$Rh(PPh_3)Cl$ π complex (**14**).[20] With the Rh catalyst, 1,2-acyloxy migration is a concerted process, requiring an activation free energy of 17.7 kcal/mol (**TS1**). In **TS1**, the Rh prefers to be anti to the acyloxy group on ACE (Figure 2). The syn pathway, in which the Rh is syn to the acyloxy, is stepwise, and is disfavored by 5.4 kcal/mol (**TS1′**). 1,3-Acyloxy migration requires a much higher activation barrier of 23.5 kcal/mol (**TS2**). This is consistent with the experimental observation where 1,2-acyloxy migration product is formed exclusively with ACE **1**.[14] The preference of 1,2-migration is also consistent with the reaction of terminal propargylic esters with other TM catalysts.

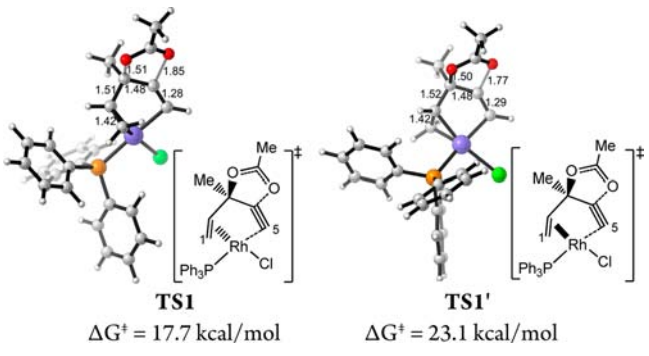

Figure 2. Two possible 1,2-acyloxy migration transition states.

The 1,2-acyloxy migration leads directly to a Rh-allyl complex **15**, in which PPh_3 is trans to the alkenyl group (C5). Complex **15** isomerizes to a more stable Rh-allyl intermediate **16**, in which the Cl is trans to the alkenyl group. We also considered other possible intermediates proposed by Rautenstrauch and others (**4**−**6**, Scheme 1). They are all higher in energy than **15** and **16** (see the Supporting Information (SI) for details).

Subsequent alkyne insertion takes place from the Rh-allyl intermediate **16** via two distinct pathways: the alkyne may insert into the Rh−C5(sp^2) bond (**TS3**) to form rhodacyclooctatriene **20**, in which the three double bonds are all conjugated (pathway I), or insert into the Rh−C1(allyl) bond (**TS5**) to form an isomeric metallacycle **23** (pathway II). The computed activation barrier of the alkyne insertion into the Rh−C5(sp^2) bond (**TS3**) is 7.4 kcal/mol lower than for insertion into the Rh−C1(allyl) bond (**TS5**, see Figure 3 for structures of the transition states). The higher activity of alkyne insertion into the Rh−C(sp^2) bond is attributed to greater orbital overlap of the HOMO of the Rh-allyl intermediate **16** and LUMO of the alkyne. As illustrated in Figure 4, the HOMO of **16** is mainly localized at the π orbital of the conjugated diene. Therefore, attack of the alkyne at the sp^2 C results in favorable orbital overlap between the diene π orbital and alkyne π^* orbital. Thus, in the (5+2) cycloaddition of ACE,

dx.doi.org/10.1021/ja4036785 | J. Am. Chem. Soc. 2013, 135, 9271−9274

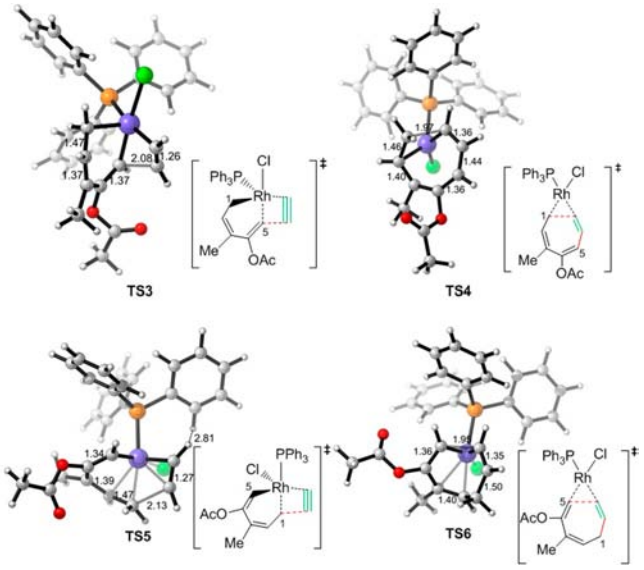

Figure 3. Optimized geometries of the alkyne insertion and reductive elimination transition states in pathway I (**TS3** and **TS4**) and pathway II (**TS5** and **TS6**).

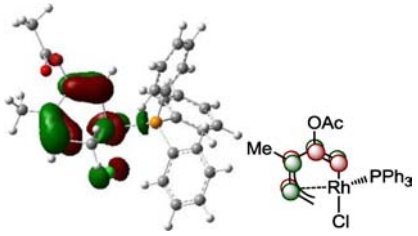

Figure 4. HOMO of rhodacyclohexadiene intermediate **16**.

the first C−C bond is formed with the alkynyl C of ACE, and the new C−C bond with the alkenyl C is formed later in the reductive elimination. In contrast, in the (5+2) reaction with VCPs, the alkyne preferentially inserts into the Rh-allyl bond and forms the first C−C bond with the alkenyl C of VCP. In the reaction with VCP, the C4−C5 bond is saturated, and the alkyne insertion into the Rh−C(allyl) bond is favorable. The different order of bond formation in the ACE reaction suggests a different regiochemical preference for the (5+2) cycloadduct that may lead to complementary products to the reactions of VCPs. The regioselectivity will be discussed in more details later. The overall barrier of alkyne insertion via **TS3** is 12.2 kcal/mol with respect to intermediate **16**. This suggests that alkyne insertion is faster than the corresponding alkyne insertion step in the reaction with VCP. It also has lower barrier than the previous 1,2-acyloxy migration step.

The rhodacyclooctatriene intermediate **20** subsequently undergoes C(sp^2)−C(sp^3) reductive elimination to form the second new C−C bond via transition state **TS4**, leading to the product π complex **21**. This step has a free energy barrier of 12.8 kcal/mol, comparable to the alkyne insertion step. Finally, **21** liberates the product and coordinates with another reactant molecule to regenerate **14** to complete the catalytic cycle. Although pathway II requires a low barrier for reductive elimination between two sp^2 C's (**23**→**TS6**, $\Delta G^{\ddagger}$ = 3.2 kcal/mol), the high barrier of alkyne insertion (**16**→**TS5**, $\Delta G^{\ddagger}$ = 19.6 kcal/mol) ruled out this pathway in the preferred catalytic cycle.

In summary, the preferred catalytic cycle of Rh-catalyzed (5+2) cycloadditions of ACE and alkynes involves three key steps: 1,2-acyloxy migration, alkyne insertion into the Rh−C(sp^2) bond in the Rh−allyl complex, and finally the C(sp^2)−C(sp^3) reductive elimination (pathway I, shown in black in Figure 1). The rate-determining step in the catalytic cycle is 1,2-acyloxy migration.

We then investigated the effects of substituents on the rate of the reaction, which is determined by the barrier of 1,2-acyloxy migration. Experimentally, electron-rich esters dramatically increase the reactivity of ACEs in the (5+2) cycloaddition.[21] The computed free energy barriers provide good agreement with the experimental reactivities of different esters (Table 1).

Table 1. Computed Relative Reaction Rates for (5+2) Cycloadditions of ACE Derivatives and Acetylene[a]

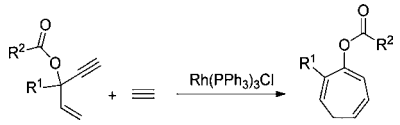

entry	R^1	R^2	$\Delta G^{\ddagger}$ (**TS1**−**14**)[b]	pred rel rate[c]	exp rel rate[c,d]
1	H	Me	20.0	0.01	no reaction
2	Me	Me	17.7	0.36	0.68
3	Me	Ph	17.1	1.00	1.00
4	Me	*p*-$Me_2NC_6H_4$	14.5	80.2	46.3

[a]See the SI for computed rates for more substrates. [b]Activation free energy (in kcal/mol) of the rate-determining 1,2-acyloxy migration step. [c]Rates are relative to the rate of entry 3. [d]Experimental relative rates from Table 1 of ref 21.

Apparently, the electron-donating group stabilizes the positive charge building up in the oxocyclic transition state (**TS1**, see the SI for NPA charge analysis). The ACE without methyl substitution at C3 (entry 1, Table 1) requires a significantly higher 1,2-migration barrier than other ACE substrates, in agreement with the low reactivity observed in experiment.[22]

The computed potential energy profile indicated the formation of the first C−C bond to form the rhodacycloocta-triene intermediate **20** is irreversible and thus is the regioselectivity-determining step.[23] Cycloadditions of ACE with unsymmetrically substituted alkynes may lead to two regioisomeric products due to the different orientations of alkyne during the alkyne insertion step (Table 2). We computed the

Table 2. Computed Regioselectivities for (5+2) Cycloadditions of ACE and Substituted Alkynes

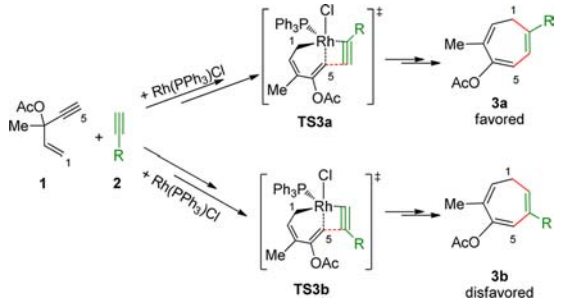

entry	R	$\Delta\Delta G^{\ddagger}$ (**TS3a**−**TS3b**)[a]	pred ratio[b]	exp ratio[b]
1	CH_2OH **24**	−4.1	>20:1	>20:1
2	TMS **25**	−2.4	>20:1	10:1

[a]Gibbs free energy differences between **TS3a** and **TS3b** in kcal/mol. [b]Ratio of **3a**:**3b**; exp ratio from Table 7 of ref 14b.

dx.doi.org/10.1021/ja4036785 | J. Am. Chem. Soc. 2013, 135, 9271−9274

differences of activation barriers of the regioisomeric alkyne insertion TSs for the reactions with propargylic alcohol **24** and trimethylsilylacetylene **25**. The predicted regioselectivities are summarized in Table 2. The regioselectivity is dominated by steric effects. In both reactions, the terminal alkyne substituent prefers to be adjacent to the metal to avoid steric repulsions around the forming C−C bond (see the SI for the structures of the regioisomeric TSs). This leads to the major regioisomeric product **3a**, in which the alkyne substituent R is distal to the first forming C−C bond, i.e., the former terminal alkynyl carbon (C5). The agreement of predicted regioselectivities with experiment[24] further validated the computed mechanism that alkyne insertion into the Rh−C(sp^2) bond is preferred.

In summary, we performed DFT calculations to explore the mechanism, reactivity, and regioselectivity in $Rh(PPh_3)_3Cl$-catalyzed intermolecular (5+2) cycloaddition of ACE and alkynes. The catalytic cycle involves an unprecedented concerted 1,2-acyloxy migration to form a rhodium-allyl intermediate, alkyne insertion into the Rh−C(sp^2) bond, and reductive elimination. The product regioselectivity is determined during formation of the first C−C bond in the alkyne insertion step. Bulkier alkyne substituent prefers to be distal to the first formed C−C bond. Our calculation predicts that the 1,2-acyloxy migration is the rate-determining step, which is consistent with higher reactivity experimentally observed for ACEs bearing an electron-rich benzoate. The significant differences between Rh-catalyzed cycloadditions of ACE and VCP disclosed here may have broad implications in understanding and development of transition-metal-catalyzed reactions.

■ ASSOCIATED CONTENT

Supporting Information

Complete ref 16, optimized geometries, and energies of all computed species. This material is available free of charge via the Internet at http://pubs.acs.org.

■ AUTHOR INFORMATION

Corresponding Author

houk@chem.ucla.edu; wtang@pharmacy.wisc.edu; xxfang@nankai.edu.cn

Notes

The authors declare no competing financial interest.

■ ACKNOWLEDGMENTS

We are grateful to the NSF (K.N.H., CHE-1059084), NIH (W.T., R01GM088285), and the Natural Science Foundation of China (X.X., 21103094) for financial support of this research. Calculations were performed on the Hoffman2 cluster at UCLA and the Extreme Science and Engineering Discovery Environment (XSEDE), which is supported by the NSF.

■ REFERENCES

(1) (a) Battiste, M. A.; Pelphrey, P. M.; Wright, D. L. *Chem. Eur. J.* **2006**, *12*, 3438. (b) Butenschön, H. *Angew. Chem., Int. Ed.* **2008**, *47*, 5287.

(2) (a) Ylijoki, K. E. O.; Stryker, J. M. *Chem. Rev.* **2013**, *113*, 2244. (b) Pellissier, H. *Adv. Synth. Catal.* **2011**, *353*, 189. (c) Harmata, M. *Chem. Commun.* **2010**, *46*, 8886. (d) Harmata, M. *Chem. Commun.* **2010**, *46*, 8904. (e) Lohse, A. G.; Hsung, R. P. *Chem. Eur. J.* **2011**, *17*, 3812.

(3) Wender, P. A.; Takahashi, H.; Witulski, B. *J. Am. Chem. Soc.* **1995**, *117*, 4720.

(4) (a) Wender, P. A.; Husfeld, C. O.; Langkopf, E.; Love, J. A. *J. Am. Chem. Soc.* **1998**, *120*, 1940. (b) Wender, P. A.; Glorius, F.; Husfeld, C. O.; Langkopf, E.; Love, J. A. *J. Am. Chem. Soc.* **1999**, *121*, 5348. (c) Wender, P. A.; Barzilay, C. M.; Dyckman, A. J. *J. Am. Chem. Soc.* **2001**, *123*, 179. (d) Wegner, H. A.; De Meijere, A.; Wender, P. A. *J. Am. Chem. Soc.* **2005**, *127*, 6530.

(5) (a) Trost, B. M.; Toste, F. D.; Shen, H. *J. Am. Chem. Soc.* **2000**, *122*, 2379. (b) Trost, B. M.; Shen, H. C. *Angew. Chem., Int. Ed.* **2001**, *40*, 2313.

(6) Zuo, G.; Louie, J. *J. Am. Chem. Soc.* **2005**, *127*, 5798.

(7) Fürstner, A.; Majima, K.; Martín, R.; Krause, H.; Kattnig, E.; Goddard, R.; Lehmann, C. W. *J. Am. Chem. Soc.* **2008**, *130*, 1992.

(8) (a) Jiao, L.; Ye, S.; Yu, Z. *J. Am. Chem. Soc.* **2008**, *130*, 7178. (b) Li, Q.; Jiang, G.; Jiao, L.; Yu, Z. *Org. Lett.* **2010**, *12*, 1332.

(9) Inagaki, F.; Sugikubo, K.; Miyashita, Y.; Mukai, C. *Angew. Chem., Int. Ed.* **2010**, *49*, 2206.

(10) (a) Ashfeld, B. L.; Miller, K. A.; Smith, A. J.; Tran, K.; Martin, S. F. *Org. Lett.* **2005**, *7*, 1661. (b) Ashfeld, B. L.; Miller, K. A.; Smith, A. J.; Tran, K.; Martin, S. F. *J. Org. Chem.* **2007**, *72*, 9018.

(11) (a) Dzwiniel, T. L.; Stryker, J. M. *J. Am. Chem. Soc.* **2004**, *126*, 9184. (b) Witherell, R. D.; Ylijoki, K. E. O.; Stryker, J. M. *J. Am. Chem. Soc.* **2008**, *130*, 2176.

(12) Tanino, K.; Shimizu, T.; Miyama, M.; Kuwajima, I. *J. Am. Chem. Soc.* **2000**, *122*, 6116.

(13) (a) Yu, Z.; Wender, P. A.; Houk, K. N. *J. Am. Chem. Soc.* **2004**, *126*, 9154. (b) Wang, Y.; Wang, J.; Su, J. C.; Huang, F.; Jiao, L.; Liang, Y.; Yang, D.; Zhang, S.; Wender, P. A.; Yu, Z. *J. Am. Chem. Soc.* **2007**, *129*, 10060. (c) Yu, Z.; Cheong, P. H. Y.; Liu, P.; Legault, C. Y.; Wender, P. A.; Houk, K. N. *J. Am. Chem. Soc.* **2008**, *130*, 2378. (d) Liu, P.; Cheong, P. H. Y.; Yu, Z.; Wender, P. A.; Houk, K. N. *Angew. Chem., Int. Ed.* **2008**, *47*, 3939. (e) Liu, P.; Sirois, L. E.; Cheong, P. H. Y.; Yu, Z.; Hartung, I. V.; Rieck, H.; Wender, P. A.; Houk, K. N. *J. Am. Chem. Soc.* **2010**, *132*, 10127. (f) Xu, X.; Liu, P.; Lesser, A.; Sirois, L. E.; Wender, P. A.; Houk, K. N. *J. Am. Chem. Soc.* **2012**, *134*, 11012. (g) Hong, X.; Liu, P.; Houk, K. N. *J. Am. Chem. Soc.* **2013**, *135*, 1456−1462. (h) Hong, X.; Trost, B. M.; Houk, K. N. *J. Am. Chem. Soc.* **2013**, *135*, 6588.

(14) (a) Shu, X.-Z.; Huang, S.; Shu, D.; Guzei, I. A.; Tang, W. *Angew. Chem., Int. Ed.* **2011**, *50*, 8153. (b) Shu, X.-Z.; Li, X.; Shu, D.; Huang, S.; Schienebeck, C. M.; Zhou, X.; Robichaux, P. J.; Tang, W. *J. Am. Chem. Soc.* **2012**, *134*, 5211.

(15) (a) Rautenstrauch, V. *J. Org. Chem.* **1984**, *49*, 950. (b) Zheng, H.; Zheng, J.; Yu, B.; Chen, Q.; Wang, X.; He, Y.; Yang, Z.; She, X. *J. Am. Chem. Soc.* **2010**, *132*, 1788. (c) Garayalde, D.; Gómez-Bengoa, E.; Huang, X.; Goeke, A.; Nevado, C. *J. Am. Chem. Soc.* **2010**, *132*, 4720.

(16) Frisch, M. J.; et al. *Gaussian 09*, revision B.01; Gaussian, Inc.: Wallingford, CT, 2010.

(17) Ribeiro, R. F.; Marenich, A. V.; Cramer, C. J.; Truhlar, D. G. *J. Phys. Chem. B* **2011**, *115*, 14556.

(18) (a) Marion, N.; Nolan, S. P. *Angew. Chem., Int. Ed.* **2007**, *46*, 2750. (b) Shu, X.-Z.; Shu, D.; Schienebeck, C. M.; Tang, W. *Chem. Soc. Rev.* **2012**, *41*, 7698.

(19) (a) Faza, O. N.; Lopez, C. S.; Alvarez, R.; de Lera, A. R. *J. Am. Chem. Soc.* **2006**, *128*, 2434. (b) Soriano, E.; Marco-Contelles, J. *Chem. Eur. J.* **2008**, *14*, 6771. (c) Soriano, E.; Marco-Contelles, J. *Acc. Chem. Res.* **2009**, *42*, 1026.

(20) The $Rh(PPh_3)_3Cl$ catalyst first undergoes ligand exchange to eliminate two PPh_3 molecules and bind to the π bonds of ACE to form **14**. This step is highly exergonic by 22.1 kcal/mol. This indicates **14** is the most stable prereaction complex.

(21) Schienebeck, C. M.; Robichaux, P. J.; Li, X.; Chen, L.; Tang, W. *Chem. Commun.* **2013**, *49*, 2616.

(22) R^1 substitution stabilizes the Rh-allyl intermediate (**15**) and thus lowers the barrier of acyloxy migration. See the SI for more details.

(23) After formation of **20**, the forward reaction barrier to form the product (**20**→**TS4**) is much lower than the reverse reaction to regenerate the alkyne (**20**→**TS3**).

(24) Computations predicted the correct major regioisomeric products for the reactions with alkynes **24** and **25**. However, the regioselectivity with **25** is slightly overestimated.